

# Excitation functions of $^3\text{He}$ -particle induced reactions on $^{101}\text{Ru}$ and $^{102}\text{Ru}$ for production of the medically interesting radionuclide $^{101\text{m}}\text{Rh}$

Ye. Skakun<sup>1,a</sup> and S.M. Qaim<sup>2</sup>

<sup>1</sup> National Science Center “Kharkiv Institute of Physics & Technology”, 61108 Kharkiv, Ukraine

<sup>2</sup> Institut für Nuklearchemie, Forschungszentrum Jülich GmbH, 52425 Jülich, Germany

**Abstract.** Using the stacked-foil technique with thin enriched ruthenium targets, excitation functions of  $^{101}\text{Ru}(^3\text{He},x)^{101\text{m}}\text{Rh}$ ,  $^{102}\text{Ru}(^3\text{He},x)^{101\text{m}}\text{Rh}$  and several other reactions were measured to study the possibility of production of the medical radioisotope  $^{101\text{m}}\text{Rh}$  in helion induced reactions. The  $^3\text{He}$ -ion energy region extended up to 34 MeV. The  $^{101}\text{Ru}(^3\text{He},x)^{101\text{m}}\text{Rh}$  reaction was found to be the most effective one. The integral thick target yield of the product radionuclide  $^{101\text{m}}\text{Rh}$  calculated from the excitation function amounts to 16.1 MBq/ $\mu\text{Ah}$  with the sum of the long-lived impurities  $^{101\text{g}}\text{Rh}$ ,  $^{102\text{m}}\text{Rh}$ , and  $^{102\text{g}}\text{Rh}$  being 0.5% at the maximum bombarding energy.

## 1 Introduction

Rhodium (Rh) belongs to the platinum (Pt) group elements. Some of the Rh-metal complexes have anti-tumor activities, similar to compounds of other elements of this group. Furthermore, Rh-labelled radiopharmaceuticals can prove to be diagnostic tools for tumor localization. Among the radioisotopes of Rh the isomer  $^{101\text{m}}\text{Rh}$  ( $T_{1/2} = 4.34$  d) has the best properties for nuclear medicine applications. Its electron capture decay to the stable  $^{101}\text{Ru}$  is followed by the intense emission (81%) of the 307 keV gamma-ray which can be observed with a  $\gamma$ -camera. Some experiments conducted earlier reported the production of  $^{101\text{m}}\text{Rh}$  using a medium-sized cyclotron. Scholz et al. [1] and Lagunas-Solar et al. [2,3] investigated the possibility of the  $^{101\text{m}}\text{Rh}$  production in the  $^{103}\text{Rh} + p$  and  $^{\text{nat}}\text{Pd} + p$  interactions at incident proton energies up to 67 and 60 MeV, respectively. Furthermore, the excitation functions of the reactions  $^{103}\text{Rh}(p,x)^{101\text{m}}\text{Rh}$  and  $^{\text{nat}}\text{Ag}(p,x)^{101\text{m}}\text{Rh}$  were measured [4,5] up to the bombarding energies 29 and 78 MeV, respectively. Thus, to day only the proton induced reactions were investigated for the production of  $^{101\text{m}}\text{Rh}$ .

In the present work the excitation functions of the reactions  $^{101}\text{Ru}(^3\text{He},x)^{101\text{m}}\text{Rh}$  and  $^{102}\text{Ru}(^3\text{He},x)^{101\text{m}}\text{Rh}$  were measured using thin targets of highly enriched ruthenium isotopes. The aim was to investigate the possibility of the production of  $^{101\text{m}}\text{Rh}$  in no-carrier form in  $^3\text{He}$ -particle induced reactions at incident energies up to 34 MeV. Moreover, excitation functions of several side reactions were measured to estimate the amount of the long-lived impurities  $^{101\text{g}}\text{Rh}$  ( $T_{1/2} = 3.3$  y),  $^{102\text{m}}\text{Rh}$  ( $T_{1/2} = 3.8$  y) and  $^{102\text{g}}\text{Rh}$  ( $T_{1/2} = 207$  d).

## 2 Experimental

The conventional stacked-foil technique and high resolution  $\gamma$ -ray spectrometry [6,7] were used for measurements of the reaction cross sections. The thin metallic foils of  $^{101}\text{Ru}$  and  $^{102}\text{Ru}$  ( $\varnothing = 16$  mm), prepared by an electrolytic deposition technique [8], were employed throughout the experiment. The

enriched material was supplied by the State Fund of Stable Isotopes (Russia). The enrichment of  $^{101}\text{Ru}$  amounted to 97.6% and of  $^{102}\text{Ru}$  to 99.0%. The surface density of the foils ranged from 2 to 5 mg  $\cdot$  cm<sup>-2</sup>. Three stacks of  $^{101}\text{Ru}$  and three of  $^{102}\text{Ru}$  were irradiated with the  $^3\text{He}$  ion beam at the compact cyclotron CV28 of the Forschungszentrum Jülich. The  $^{101}\text{Ru}$  stacks covered the beam energy regions 34  $\rightarrow$  7, 34  $\rightarrow$  21 and 24  $\rightarrow$  12 MeV, and  $^{102}\text{Ru}$  stacks the regions 34  $\rightarrow$  7, 34  $\rightarrow$  19 and 24  $\rightarrow$  9 MeV. Titanium and aluminium foils (all supplied by Goodfellow Metals, England) were inserted between the ruthenium foils: the former for monitoring  $^3\text{He}$ -particle beam and the latter for the beam energy absorption along the stack.

The product activities in Ru samples and Ti monitor foils were measured with a HPGe-detector whose efficiency calibration was done using the standard radioactive sources  $^{57}\text{Co}$ ,  $^{133}\text{Ba}$ ,  $^{137}\text{Cs}$ ,  $^{152}\text{Eu}$ ,  $^{226}\text{Ra}$  and  $^{241}\text{Am}$ . The activities of all samples were periodically measured over a period of 2 months, watching the half-life and choosing the best cooling time and the minimum dead time to determine each activity correctly. Absolute yields of 9 radioisotopes ( $^{43,44\text{m},46,47,48}\text{Sc}$ ,  $^{48}\text{V}$ ,  $^{48,49,51}\text{Cr}$ ) in the  $^3\text{He} + ^{\text{nat}}\text{Ti}$  interactions were measured for both beam monitoring and checking the  $^3\text{He}$ -particle energy degradation using cross section values published in [9, 10]. The activities of the Ru +  $^3\text{He}$  interaction products were also observed and measured in each densely packed Al foil, giving the possibility to determine the number of residual nuclei leaving the thin ruthenium foils, to be able to introduce corrections in the cross section calculations. The incident particle energy for each Ru target was determined by a code calculating the energy degradation along the stack using the range-energy expression [11].

The radionuclide  $^{101\text{m}}\text{Rh}$  is produced in  $^{101}\text{Ru}$  and  $^{102}\text{Ru}$  targets via the reactions  $^{101}\text{Ru}(^3\text{He}, p2n + dn + t)^{101\text{m}}\text{Rh}$  and  $^{102}\text{Ru}(^3\text{He}, p3n + d2n + tn)^{101\text{m}}\text{Rh}$ , respectively. This isomer is also produced by an indirect way during the decay of its precursor  $^{101}\text{Pd}$  ( $T_{1/2} = 8.47$  h), resulting from the reactions  $^{101}\text{Ru}(^3\text{He}, 3n)^{101}\text{Pd}$  and  $^{102}\text{Ru}(^3\text{He}, 4n)^{101}\text{Pd}$ , both of which have relatively high cross sections.

We calculated the thin target reaction cross sections for the production of  $^{102\text{m}}\text{Rh}$ ,  $^{102\text{g}}\text{Rh}$ ,  $^{101\text{m}}\text{Rh}$  (cumulative), and  $^{101\text{g}}\text{Rh}$

<sup>a</sup> Present author, e-mail: skakun@kipt.kharkov.ua

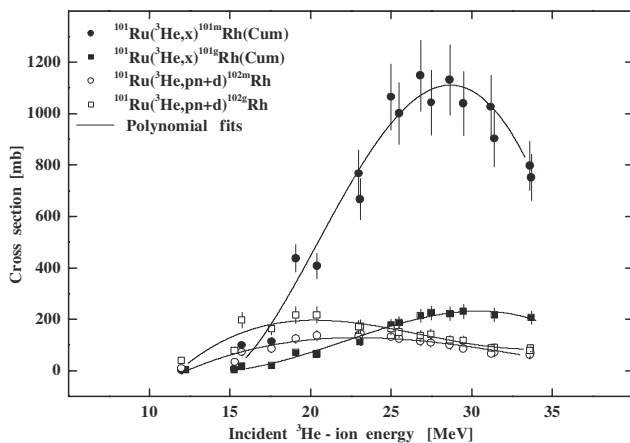


**Fig. 1.** Measured (points) excitation functions of the reactions producing  $^{101m,g}\text{Rh}$  and  $^{102m,g}\text{Rh}$  isomers on  $^{101}\text{Ru}$  target. The curves are polynomial fits.

(cumulative), using the conventional activation equation taking into account their decay during the irradiation, cooling and measurement time.

### 3 Results

The measured excitation functions of  $^{101}\text{Ru}(^3\text{He},x)$  reactions producing the radionuclides  $^{101m}\text{Rh}$ ,  $^{101g}\text{Rh}$ ,  $^{102m}\text{Rh}$ , and  $^{102g}\text{Rh}$  are shown in figure 1. The dark circle points correspond to the  $^{101}\text{Ru}(^3\text{He},x)^{101g}\text{Rh}$  (Cum) process of cumulative formation of the product, i.e., the sum of the reactions  $^{101}\text{Ru}(^3\text{He},p2n + dn + t)^{101g}\text{Rh}$  (direct way) and  $^{101}\text{Ru}(^3\text{He},3n)^{101}\text{Pd} \rightarrow ^{101m}\text{Rh}$  (indirect way). The excitation function of the process  $^{101}\text{Ru}(^3\text{He},x)^{101m}\text{Rh}$  (Cum) contributed by the reactions  $^{101}\text{Ru}(^3\text{He},p2n + dn + t)^{101m}\text{Rh}$  (direct way) and  $^{101}\text{Ru}(^3\text{He},x)^{101m}\text{Rh}(\text{Cum}) \rightarrow ^{101g}\text{Rh}$  is presented with the dark square points on the same graph. The excitation functions of the reactions  $^{101}\text{Ru}(^3\text{He},pn + d)^{102m}\text{Rh}$  and  $^{101}\text{Ru}(^3\text{He},pn + d)^{102g}\text{Rh}$  for the production of the isomeric pair  $^{102m,g}\text{Rh}$  are displayed by the open circles and squares, respectively. Since  $^{102}\text{Rh}$  is a blocked nucleus from both sides of the valley of stability the cross sections for its production are independent ones.

Analogously, for the  $^{102}\text{Ru}$  target the reactions  $^{102}\text{Ru}(^3\text{He},p3n + d2n + tn)^{101m}\text{Rh}(\text{directway}) + ^{102}\text{Ru}(^3\text{He},4n)^{101}\text{Pd} \rightarrow ^{101m}\text{Rh}$  (indirect way) contribute to the cumulative production of  $^{101m}\text{Rh}$  and the reactions  $^{102}\text{Ru}(^3\text{He},p3n + d2n + tn)^{101g}\text{Rh}$  (direct way) and  $^{102}\text{Ru}(^3\text{He},x)^{101m}\text{Rh}(\text{Cum}) \rightarrow ^{101g}\text{Rh}$  to the cumulative production of  $^{101g}\text{Rh}$  (the dark points in fig. 2). The open circles and squares depict the measured cross sections of the reactions  $^{102}\text{Ru}(^3\text{He},p2n + dn + t)^{102m}\text{Rh}$  and  $^{102}\text{Ru}(^3\text{He},p2n + dn + t)^{102g}\text{Rh}$ , respectively, for the production of the isomeric pair  $^{102m,g}\text{Rh}$ .

Of all the reactions presented in figures 1 and 2 the process  $^{101}\text{Ru}(^3\text{He},x)^{101m}\text{Rh}$  (Cum) is distinctive: its cross section reaches  $\sim 1100\text{mb}$  at the incident  $^3\text{He}$ -ion energy of 28 to 29 MeV and apparently it is the most effective route to produce

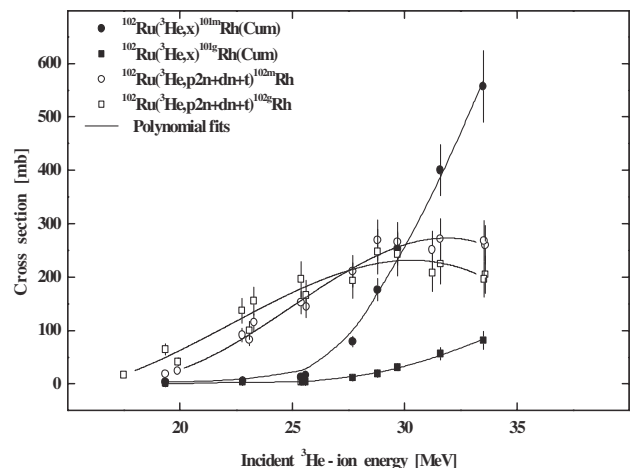


**Fig. 2.** Measured (points) excitation functions of the reactions producing  $^{101m,g}\text{Rh}$  and  $^{102m,g}\text{Rh}$  isomers on  $^{102}\text{Ru}$  target. The curves are polynomial fits.

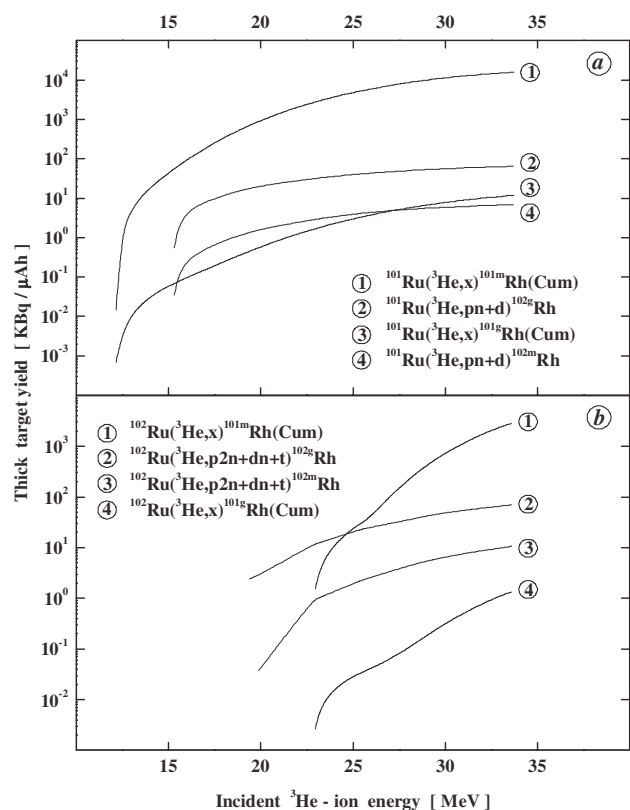


**Fig. 3.** Integral yields of the  $^{101m,g}\text{Rh}$  and  $^{102m,g}\text{Rh}$  isomers formed in  $^3\text{He}$ -particle induced reactions on the enriched  $^{101}\text{Ru}$  (graph *a*) and  $^{102}\text{Ru}$  (graph *b*) targets, calculated from the measured reaction cross sections.

the medical radioisotope  $^{101m}\text{Rh}$ . The cross sections of other reactions have lower values in the bombarding energy region studied.

Individual members of pairs of reactions occurring in  $^{101}\text{Ru}$  and  $^{102}\text{Ru}$  targets but resulting in the same product nucleus differ considerably from one another in both energy dependence and absolute values of cross sections. The cross

contamination corrections in the production cross sections of the four studied isomers ( $^{101\text{m}}\text{Rh}$ ,  $^{101\text{g}}\text{Rh}$ ,  $^{102\text{m}}\text{Rh}$ , and  $^{102\text{g}}\text{Rh}$ ) on both targets were therefore energy dependent. The smallest values ( $\sim 1\%$  and less) were observed for the reactions  $^{101}\text{Ru}(^3\text{He},x)^{101\text{m,g}}\text{Rh}$  and the largest ones (up to 40% at low bombarding energies in spite of the very high target enrichment) for the reaction  $^{102}\text{Ru}(^3\text{He},x)^{101\text{m}}\text{Rh}$ . So the cross contamination corrections were most significant in the near threshold region.

The thick target yields of the medical radioisotope  $^{101\text{m}}\text{Rh}$  and the other undesired radionuclides calculated from the "cumulative excitation functions" of the  $^3\text{He}$ -particle induced reactions on  $^{101}\text{Ru}$  and  $^{102}\text{Ru}$  targets are presented in figure 3. The cumulative yields of  $^{101\text{m}}\text{Rh}$  in the  $^3\text{He}$ -particle induced reactions on  $^{101}\text{Ru}$  and  $^{102}\text{Ru}$  amount to 16.1 MBq/ $\mu\text{Ah}$  and 2.9 MBq/ $\mu\text{Ah}$ , respectively, at 34 MeV beam energy.

The sum of the long-lived impurities  $^{101\text{g}}\text{Rh}$ ,  $^{102\text{m}}\text{Rh}$  and  $^{102\text{g}}\text{Rh}$  amounts to 0.5% in case of  $^{101}\text{Ru}$  and 2.9% for  $^{102}\text{Ru}$  target.

The medical radionuclide  $^{101\text{m}}\text{Rh}$  can thus be produced in no-carrier-added form in sufficient quantity and good radionuclidic purity in the  $^{101}\text{Ru}(^3\text{He},x)^{101\text{m}}\text{Rh}$  (Cum) reaction using  $^3\text{He}$ -ion beam of a medium-sized cyclotron.

We thank Prof. H.H. Coenen for his support of this project, the cyclotron operation crew for the help in performing target irradiation, Mr St. Spellerberg for his experimental assistance and the Deutsche Forschungsgemeinschaft (DFG, Bonn) for financial support.

## References

1. K.L. Scholz, V.J. Sodd, J.W. Blue, *Int. J. Appl. Radiat. Isot.* **28**, 207 (1977).
2. M.C. Lagunas-Solar, M.J. Avila, P.C. Johnson. *Int. J. Appl. Radiat. Isot.* **35**, 743 (1984).
3. M.C. Lagunas-Solar, S.R. Wilkins, D.W. Paulson, *J. Radioanal. Chem.* **68**, 245 (1982).
4. A. Hermanne, M. Sonck, A. Fenyvesi, L. Daraban. *Nucl. Instrum. Meth. Phys. Res. B* **170**, 281 (2000).
5. M.S. Uddin, M. Hagiwara, M. Baba, F. Tárkányi, F. Ditroi. *Appl. Radiat. Isot.* **62**, 533 (2005).
6. S. Sudár, F. Cserpák, S.M. Qaim, *Appl. Radiat. Isot.* **56**, 821 (2002).
7. Ye. Skakun, S.M. Qaim, *Appl. Radiat. Isot.* **60**, 33 (2004).
8. A.P. Kljucharev, L.I. Kovalenko, L.G. Lishenko, V.N. Medjanik, T.S. Nazarova, A.A. Rozen., *Thin Foils of Metal Isotopes. Preparation Methods* (Energoizdat, Moscow, 1981).
9. F. Tárkányi, S. Takács, K. Gul, A. Hermanne, M.G. Mustafa, M. Nortier, P. Obložinský, S.M. Qaim, B. Scholten, Yu.N. Shubin, Y. Zhuang, Ch. 4. Beam monitor reactions, in *Charged-Particle Cross Section Database for Medical Radioisotope Production: Diagnostic Radioisotopes and Monitor Reactions*, IAEA-TECDOC-1211 (IAEA, Vienna, 2001), p. 49.
10. Ditrói, F. Tárkányi, M.A. Ali, L. Ando, S.-J. Heselius, Yu. Shubin, Zhuang Youxiang, M.G. Mustafa, *Nucl. Instrum. Meth. Phys. Res. B* **168**, 337 (2000).
11. F. Williamson, J.P. Boujot, J. Picard, *Tables of Range and Stopping Power of Chemical Elements for Charged Particles of Energy 0.05 to 500 MeV*, Report CEA-R3042 (Saclay, 1966).